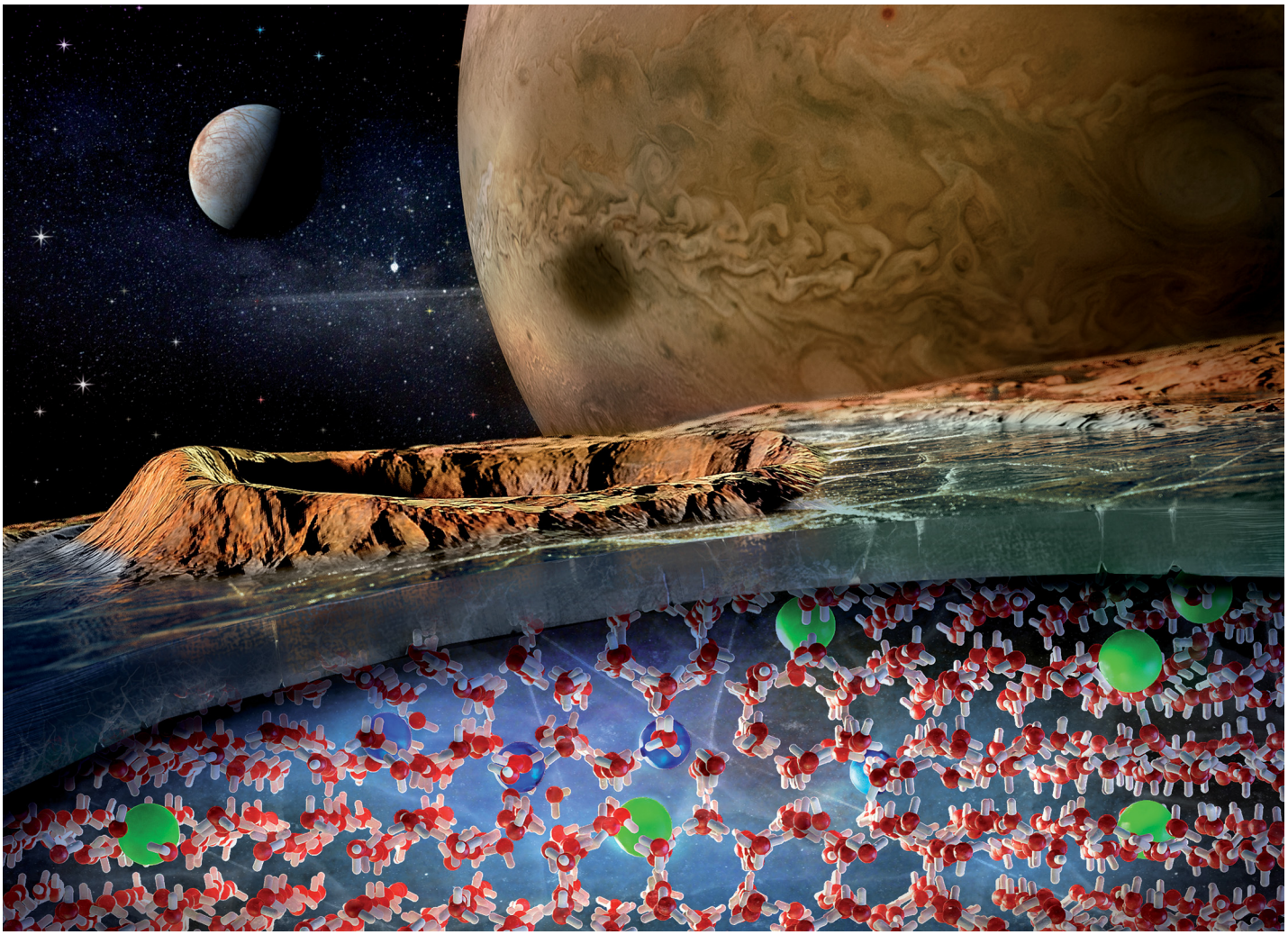

Showcasing research from the Groups of Prof. M. M. Conde at Polytechnic University of Madrid (Spain) and Prof. P. Gallo at Roma Tre University (Italy).

Spontaneous NaCl-doped ices I_h, I_c, III, V and VI. Understanding the mechanism of ion inclusion and its dependence on the crystalline structure of ice

This work shows the inclusion of Cl^- and Na^+ ions in ice from salt using molecular dynamics simulations, in agreement with the experimental evidence found in the literature for the interior of the Jupiter icy moons. The results reveal the spontaneous growth of a new ice doped phase and the formation of a brine rejection phase in all ices studied.

As featured in:

See M. M. Conde, P. Gallo *et al.*, *Phys. Chem. Chem. Phys.*, 2021, **23**, 22897.

ROYAL SOCIETY OF CHEMISTRY

rsc.li/pccp

Registered charity number: 207890

PCCP

PAPER

View Article Online
View Journal | View Issue

Cite this: *Phys. Chem. Chem. Phys.*, 2021, **23**, 22897

Spontaneous NaCl-doped ices I_h, I_c, III, V and VI. Understanding the mechanism of ion inclusion and its dependence on the crystalline structure of ice†

M. M. Conde, *[a] M. Rovere[b] and P. Gallo *[b]

Received 11th June 2021,
Accepted 15th August 2021

DOI: 10.1039/d1cp02638k

rsc.li/pccp

Direct coexistence simulations on a microsecond time scale have been performed for different types of ice (I_h, I_c, III, V, and VI) in contact with a NaCl aqueous solution at different pressures. In line with the previous results obtained for ice I_h [Conde *et al.*, *Phys. Chem. Chem. Phys.*, 2017, **19**, 9566–9574], our results reveal the spontaneous growth of a new ice doped phase and the formation of a brine rejection phase in all ices studied. However, both the preferential incorporation of ions into the ice lattice and the inclusion mechanisms depend on the crystalline structure of each ice. This work shows the inclusion of Cl^- and Na^+ ions in ice from salt using molecular dynamics simulation, in agreement with the experimental evidence found in the literature. The model used for water is TIP4P/2005. For NaCl we employ a set of potential parameters that uses unit charges for the ions.

1 Introduction

Since the discovery in recent years of icy satellites and the existence of salty oceans in the interior of this type of celestial bodies[1–4] the study of the water-salt system is receiving much attention, with the special focus on the doping processes of the ice structures. These ice-doping processes are the main argument to explain the different electrical properties found in these icy bodies. Ice-doping events are not only interesting on a planetary level, there are also other processes related to climate change[5–7] and desalination processes[8–10] where ice doping plays an important role.

The presence of a small amount of ion dopants in the solid structure of ice is already sufficient to modify its electrical properties. In particular, different experimental studies reveal how the inclusion of ions in the ice lattice modifies the dielectric properties of ice by increasing its static conductivity.[11] The inclusion of ion dopants causes the appearance of Bjerrum defects.[12] Depending on the type of ion, its inclusion in the solid structure can cause an increase or decrease in conductivity. Due to the enormous interest in nature for its abundance and properties, we will focus our study on the ions that come from NaCl salt. The presence of Cl^- ions incorporated into the ice structure provokes the creation of Bjerrum L defects favoring an increase in conductivity.[11,12]

In the 1960s, Gross *et al.*[13–15] performed numerous experimental studies explaining the role of ionic impurities found in ice on the electrical properties of ice. In 1965 Jaccard[16] explained the mechanism of the electrical conductivity of ice through the creation of Bjerrum defects. Other authors continued to investigate these ice doping processes, such as Young and Salomon[17] studying ice doped with HCl and later Kelly and Salomon[18] evaluating the dielectric behaviour of ice doped with different NaOH concentrations. Moreover, Seidensticker and Longini[19] analyzed the impurity effects on ice in presence of hydrogen fluoride and ammonia. However, it was not until the last few years that interest in these processes had reawakened. Bove and co-workers[20,21] presented several studies on salty ice VII under pressure and recently Rozsa and Galli[22] have reported first-principles molecular dynamics simulations of different ions (Li^+, K^+, Na^+ and Cl^-) in liquid water at extreme conditions (11 GPa, 1000 K).

Nevertheless, the details of the inclusion mechanisms of the different ions doping the ice structure have not been fully explored. In 2017, we carried out a detailed study using molecular dynamics simulations on the inclusion mechanism of a NaCl-doped ice.[23] At seawater conditions, we observed the brine rejection phenomenon and the spontaneous growth of an ice slab doped by Cl^- and Na^+ ions. We found that Cl^- ions substitutes not one but two water molecules in the lattice and that Na^+ ions occupy interstitial sites.

[a] *Departamento de Ingeniería Química Industrial y Medio Ambiente, Escuela Técnica Superior de Ingenieros Industriales, Universidad Politecnica de Madrid, 28006 Madrid, Spain. E-mail: maria.mconde@upm.es*
[b] *Dipartimento di Matematica e Fisica, Università Roma Tre, Via della Vasca Navale 84, 00146 Roma, Italy. E-mail: paola.gallo@uniroma3.it*

† Electronic supplementary information (ESI) available: Movies of MD trajectory of NaCl-doped ices I_h, I_c, III, V and VI. See DOI: 10.1039/d1cp02638k

In view of these findings and considering that when the pressure increases other stable phases of ice can appear, we proceeded here one step further in understanding doping processes and the mechanisms of ion inclusion. In the present work we study the role of pressure and the different crystalline structures of ice on doping processes for systems formed by a slab of ice and an aqueous solution of NaCl. We focus on studying ices I_c, III, V and VI. Likewise, we again analyze the doping process for ice I_h from an aqueous solution at a concentration above seawater conditions to evaluate the impact of the salt concentration in the aqueous solution on the ice doping.

The paper is structured as follows. In Section 2 we describe the methodology that we used in our simulations. In Section 3 we present the results obtained for each of the ice studied. We perform an exhaustive study for each ice analyzing different factors such as spontaneous doping, the preferential occupation of ions in the solid lattice and the inclusion mechanisms, among others. Finally, Section 4 summarizes the main conclusions obtained.

2 Methodology

In our previous work[23] we studied the dynamics and evolution of the ice-doping process produced when a slab of ice I_h is in contact with an aqueous solution of NaCl at different degrees of subcooling and at temperatures above the eutectic formation temperature. We observed the spontaneous NaCl-doped ice at seawater conditions when the ice phase exposed to the interface was the common ice phase I_h.

The interest in ice-doping processes extends not only to the ice phase I_h but also to other ice phases stable at high pressures that are postulated as the phases that may exist in planetary conditions, such as ice bodies with salty oceans. Thus, in this work we will study the process of doping ice for the ice I_h at higher concentrations than seawater conditions, for the metastable phase I_c at the same pressure and temperature conditions as ice I_h and for the stable ice phases at high pressures III, V and VI.

For our study, we will consider the equilibrium temperature for each ice phase obtained by simulation from the works of Conde *et al.*[24,25] and Zaragoza *et al.*[26] using the TIP4P/2005 water model. This model correctly describes many of the properties of water, including a qualitative description of the phase diagram. In agreement with the experimental diagram, the model predicts the ice phase I_h as the stable phase at atmospheric pressure and the I_c phase as a metastable phase under the same conditions. The ices III, V and VI occupy a region of stability within the phase diagram at increasingly higher pressures, respectively. Currently, TIP4P/2005 is considered one of the best models of potential for water in the literature. The Table 1 collects the melting temperatures of each pure ice in the region of the diagram where these phases are stable.

Table 1 Melting temperatures as obtained from direct coexistence simulations by Conde *et al.*[24,25] for the ices I_h, III, V and VI, and by Zaragoza *et al.*[26] for the ice I_c at different equilibrium pressures studied using the TIP4P/2005 water model. In parentheses the error bar is given

Ice	I_h	I_c	III	V	VI
p (bar)	1	1	3500	7000	12 000
T_m (K)	249(3)	249(3)	240(4)	241(3)	267(3)

Regardless of the ice phase studied, we followed the same methodology to generate the initial configuration as in the previous work.[23] A slab of ice is in contact with a solution of NaCl. For the ice I_h, we exposed the secondary prismatic plane $(1\bar{2}10)$ at the interface because it is the plane with the fastest dynamics.[27,28] For the rest of the ices we chose plane (100) because to our knowledge there are no studies about the growth rate. The number of molecules in the ice slab depends on the size of the unit cell of each phase and we replicate the unit cell until we obtain a solid phase around 2000 molecules. Finite size effects can be considered negligible for this system size.[29] For the ices I_h, I_c and VI with full proton disordered and for the ices III and V with partial proton disordered, we used the algorithm of Buch *et al.*[30] to generate a starting configuration that satisfies the Bernal–Fowler rules with a dipolar moment close to zero.[31] The initial solid configurations were equilibrated for about 50 ns at the equilibrium pressure for each ice allowing the three different sides of the simulation box to fluctuate independently to avoid stress in the solid lattice. Once all the ices are in equilibrium, each solid phase is replicated four times in the direction x and it is completely melted to generate a fluid phase with the same box dimensions on the sides y and z, allowing its subsequent assembly. In the next step, the Cl^- and Na^+ ions necessary to have a NaCl solution in the fluid phase are incorporated. We choose in all cases a concentration of 1 M. The number of ion pairs varies for each system depending on the number of water molecules in the fluid phase as well as the pressure selected. Once the ions are introduced, we performed a Np_xT simulation about 50 ns to equilibrate the NaCl(aq) phase. The Table 2 shows the number of initial molecules for each system at the beginning of the simulations. The last step consists of the assembly of both phases and a final short equilibration run (20 ps) to have equilibrium at the interface before starting the brine rejection simulations. All systems are formed by a slab of ice which acts as a seed crystal in contact with a liquid water phase containing

Table 2 Number of molecules for the phase of ice and the NaCl aqueous solution for the different systems studied in this work at the beginning of the simulations. For each system the concentration of the solution is given in terms of molarity, M (mol L^{-1}) and molality, m (mol kg^{-1})

System	n_{ice}	$n_{water}^{solution}$	$n_{NaCl}^{solution}$	M	m
I_h/NaCl(aq)	2000	8000	146	1.0	1.0
I_c/NaCl(aq)	2016	8064	147	1.0	1.0
III/NaCl(aq)	2592	10 368	171	1.0	0.9
V/NaCl(aq)	2100	8400	130	1.0	0.9
VI/NaCl(aq)	2160	8640	126	1.0	0.8

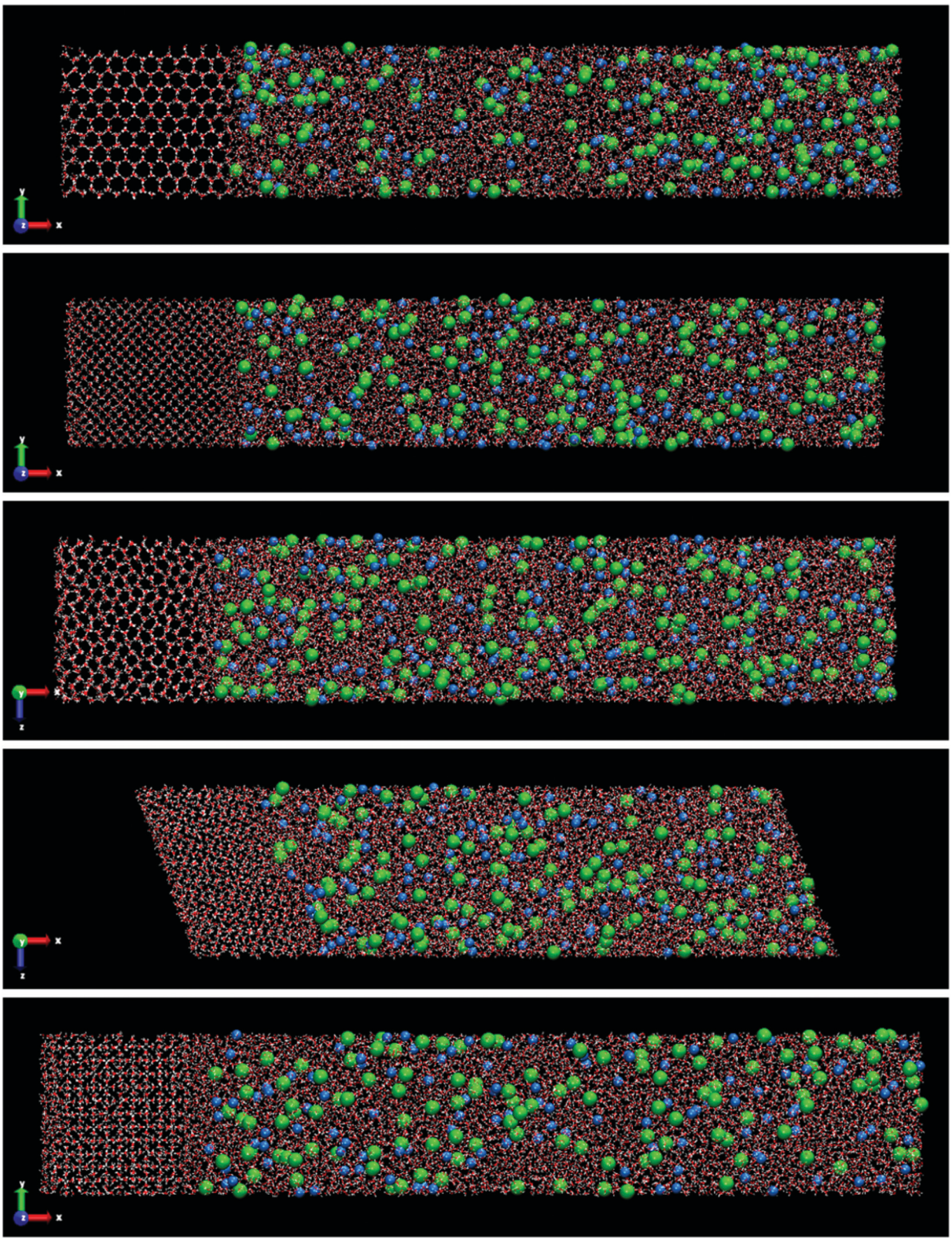

Fig. 1 Snapshots of the initial configurations for the systems formed by a slab of ice and a NaCl aqueous solution. In order from top to bottom: ices I_h, I_c, III, V and VI. Water molecules are plotted in red and white color, Cl^- ions are plotted as green spheres and Na^+ ions as blue spheres. The size of the ions is enlarged with respect to the water molecules for a clearer visualization.

Na^+ and Cl^- ions in solution with an initial salt concentration of 1 M.

The main difference of each system, in addition to the number of water molecules and ions that form it, it is the shape of the simulation box. The geometry of the simulation box is determined by the crystalline structure of the ice. Thus, for ice I_h the simulation box is orthorhombic (note that for ice I_h with hexagonal symmetry it is possible to use an orthorhombic cell[11]). For the other ices, we use a simulation box with geometry cubic for ice I_c, tetragonal for ice III, monoclinic for ice V and for ice VI a box of tetragonal symmetry. The NaCl aqueous solution adapts to the shape of the box for each ice.

We use samples with a very large size to reduce significantly the stochastic nature of the direct coexistence simulations.[29] In addition, a large fluid phase size (more than 8000 molecules for all systems) gives us the possibility, in the case of spontaneous doping, to obtain a greater number of ions in the solid lattice and thus a better statistics of the results. The idea is to put a small solid seed and grow it as much as possible. In Fig. 1 all the initial configurations used in this work for the different systems studied are shown.

Recently, we observed for the ice I_h phase that the concentration of dopants in ice increased as the degree of subcooling is higher.[23] Moreover, we observed that at temperatures close to the melting point of the ice, the Na^+ ions did not incorporate into the crystalline lattice of the ice and remained in the solution. It was necessary to lower the temperature to observe the inclusion of Na^+ ions in the solid lattice. For Cl^- ions, even at temperatures close to the melting point, the ice doped by this ion was observed. Following these results, in the present work we choose the system temperature of 20 K below the melting point because that was the temperature that gave us a number of ion inclusions similar to the experimental values in our previous study of ice I_h and for this study we kept the same temperature also for the other ices. According to the water–NaCl phase diagram, the range of temperatures where it is possible to study the equilibrium between ice and solution must be below the melting point of ice and above the eutectic point. The pressure chosen for each system was the pressure at which Conde and co-workers determined the melting point of each pure ice by direct coexistence.[24–26] Table 3 shows the initial conditions of pressure and temperature for each system studied. The degree of subcooling chosen in all cases was $\Delta T = -20$ K, where ΔT is the difference between the temperature of the system and the melting temperature of each ice.

Table 3 Initial conditions of pressure and temperature for the different systems studied in this work. ΔT is the difference between the temperature of the system (T) and the melting temperature (T_m) for each ice phase studied and the water model selected

System	p (bar)	T (K)	ΔT (K)
I_h/NaCl(aq)	1	229	−20
I_c/NaCl(aq)	1	229	−20
III/NaCl(aq)	3500	220	−20
V/NaCl(aq)	7000	221	−20
VI/NaCl(aq)	12 000	247	−20

Table 4 Potential parameters of TIP4P/2005 water model[37] and NaCl model.[38] The parameters C_6 and C_{12} are given in kJ mol^{-1} nm^6 and kJ mol^{-1} nm^{12}, respectively. The value of the charge, q, is expressed in e units

Site	C_6	C_{12}	q
O	0.30798×10^{-2}	0.30601×10^{-5}	—
H	—	—	+0.5564
M	—	—	−1.1128
Na^+	—	0.83200×10^{-7}	+1
Cl^-	—	0.52000×10^{-4}	−1
Na^+–O	0.08000×10^{-2}	2.09430×10^{-7}	—
Cl^-–O	0.15000×10^{-2}	1.64480×10^{-5}	—

For all direct coexistence simulations of the present work, we employ the Np_xT ensemble.[29,32] In this ensemble, the pressure is applied in the direction perpendicular to the interface (for all systems studied corresponds to the x-axis). To perform all simulations, we use the molecular dynamics package GROMACS (version 4.5.5).[33] Periodic boundary conditions were employed in the three directions of space. Nosé–Hoover thermostat[34,35] with a relaxation time of 2 ps was used to fix the temperature. Parrinello–Rahman barostat[36] was used to keep the pressure constant with a relaxation time of 2 ps. The time-step used in the direct coexistence simulations was 2 fs. The length of each direct coexistence simulation was on the microsecond scale depending on the type of system, going from 3 microseconds for ices I_h and I_c to 5 microseconds for ices III, V and VI.

As it was previously mentioned, we used the well-known rigid and nonpolarizable TIP4P/2005 potential[37] to describe the interactions of water molecules in our systems ice/NaCl(aq). In line with our previous work[23] and in order to be able to compare the results on spontaneous doping and quantity of doping ions, we used the parameters proposed by Vega and co-workers[38] for the ion–water and ion–ion interactions, which reproduce the solubility of NaCl in water in very good agreement with the experimental one. The potential parameters of TIP4P/2005 water and NaCl models are given in Table 4. There are other more recent potential models with scaled charges in the literature,[39,40] we use this potential with unit charges for the ions to compare with our previous results. The geometry of the water molecules was enforced using constraints. The real part of the Coulombic potential and the Lennard-Jones part of the potential were truncated both at 8.5 Å. Ewald sums were used to deal with electrostatics interactions.[41] The width of the mesh was 1 Å and we used a fourth-order polynomial.

3 Results

We start analyzing the results of the simulations performed by direct coexistence for the five systems studied containing ice I_h, I_c, III, V and VI as solid phase at $\Delta T = -20$ K and the pressure selected in each system. The evolution of the potential energy as a function of time for each system along the simulation is shown in Fig. 2. For all systems studied at the same degree of subcooling, we observe a decrease in the potential energy indicating the growth of an ice slab. In all cases, long time

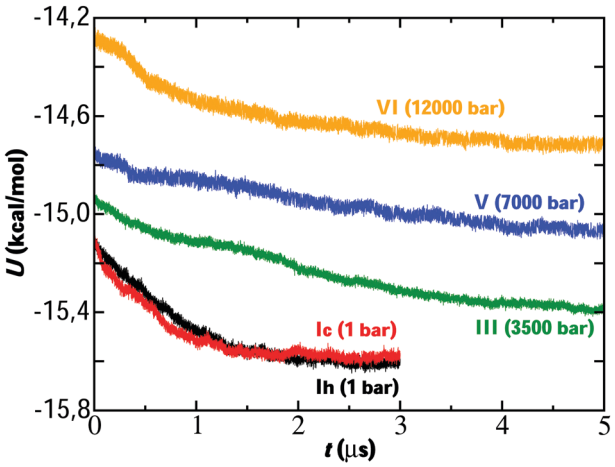

Fig. 2 Evolution of the potential energy as a function of time (on the microsecond time scale) obtained at $\Delta T = -20$ K for the systems ice/NaCl(aq) studied in this work. ΔT is the difference between the melting temperature for each ice (T_m) using the TIP4P/2005 water model and the temperature of system studied (T). The pressure to which the direct coexistence simulations have been performed for each ice system is indicated in parentheses.

simulations on a microsecond scale were necessary to carry out the growth of the solid phase.

The evolution of potential energy allows us to understand the growth velocity of the ice phase. Thus, in view of the results, we observe how the growth rate is different depending on each ice. For example, for the ice I_h and I_c we see how the energy decreases until reaching a final plateau indicating that the system has reached the state of equilibrium. Initially, a very fast decrease in potential energy is observed for these ices until gradually reaching the plateau. Considering our previous work,[23] if we compare the evolution of the energy for the system of ice I_h starting from two different initial concentrations for the NaCl solution (0.599 M in the previous work and 1 M in this work) it is observed that the growth rate is similar. Analogously, ice VI first presents a rapid fall and then its evolution is slow until it reaches the plateau. For ices III and V the fall in potential energy occurs more slowly and after simulating 5 microseconds, the final state of equilibrium is not reached. However, the portion of ice grown is sufficient for our study about ice-doping.

These results follow the trend of the growth rates obtained by Conde *et al.*[24] for simulations of direct coexistence of pure ices in the absence of salt. Conde *et al.*[24] revealed how the growth rates of ice III and V are slightly higher than those of ice I_h. A possible explanation for these differences in growth rates is due to the fact that ices III, V and VI present a much more complex structure than ice I_h. In the ice I_h all the water molecules are connected in a tetrahedral lattice and all the molecules are topologically equivalent. This is not the case for ices with more complex structures where not all molecules are topologically equivalent.[11] The growth of ice from pure liquid water is much faster than from a NaCl solution and this leds an increase of the simulation time by an order of magnitude. For the pure water system, a noticeable growth of the ice phase could be observed in around 20 ns even for more complex ice phases such as ice III or ice V.[24] Instead, from a NaCl solution, the simulation time necessary to observe that same ice growth rises to the scale of microseconds, so almost two orders of magnitude longer.

Fig. 3 shows the final snapshots for the systems studied. Each instantaneous configuration was taken at 3 microseconds for the systems formed by ice I_h and I_c, and 5 microseconds for the systems formed by ices III, V and VI. This time difference is due to the different growth rate mentioned above. As it can be seen in Fig. 3, the shape of the simulation box for the ice-solution systems is different depending on the symmetry of each ice. For ice I_h and I_c a frontal view of the *XY* plane is shown. For ice III and V the *XZ* projection is the front view. The different choice in the projection of the plane only addresses visualization issues about the type of simulation box shown, as in the case of the monoclinic box of the ice V, or a clearer visualization of the crystalline structures as the pentagonal rings of the ice III. These final snapshots show not only the growth of ice, as confirmed by the evolution of the potential energy, but also the spontaneous doping of Cl^- and Na^+ ions produced in all the ice phases studied besides the brine rejections.

In the ESI† of this work, the trajectory movies of each system are included. In these movies, the growth of ice and spontaneous doping of ions in the solid lattice are clearly observed. Already from a visual inspection we can see that the spontaneous doping of Na^+ and Cl^- ions, previously observed for direct coexistence molecular dynamics simulations of ice I_h, is obtained for all the ices investigated, not withstanding the more complex structures that they have. In fact, while in a previous work[24] there was evidence that it was possible to grow pure ice by direct coexistence of complex ice phases such as ices III, V and VI, spontaneous doping is much more complex and here we show it for the first time in a study by molecular dynamics simulations. Similarly to what we observed for ice I_h at seawater conditions,[23] the portion of doped ice for all systems corresponds to the new ice-grown phase, while the initial solid seed is pure ice. Notice that for the configuration of the Fig. 3 of the system formed by ice VI there are no ions incorporated in the initial ice slab. The Na^+ ion observed in the Fig. 3 (bottom) to the left of the final configuration of ice VI corresponds to the new grown ice slab because the box has shifted. Likewise, a repetition pattern has not been found in the distribution of the ions along the solid lattice. The ions appear randomly located in the new slab of doped ice. We observed the doped ices during all the duration of the simulations, and they all look perfectly stable. The Cl^- ions remain always in the same position while Na^+ ions move a bit locally both when they are interstitial and when they are substitutional and it can be seen in the movies. The ice around the ions is unaltered.

For ice I_h the number of Cl^- ions that are incorporated into ice is greater than Na^+ ions. This preferential doping is in agreement with the results obtained previously for a system with different starting concentrations[23] and in agreement with

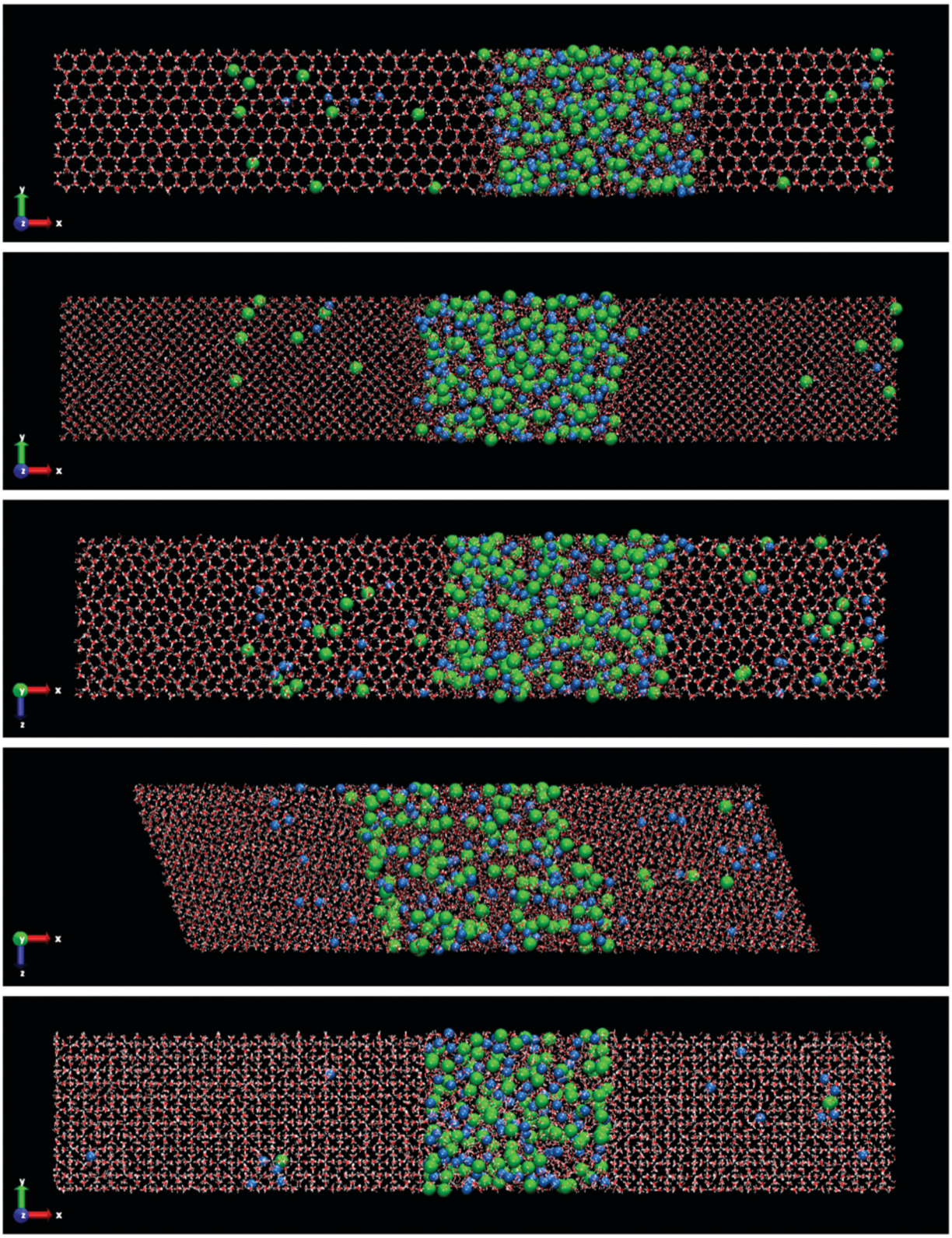

Fig. 3 Snapshots of the final configurations obtained by direct coexistence simulations for the systems formed by a slab of ice and a NaCl aqueous solution at the temperature studied ($\Delta T = -20$ K) and at different pressures depending on the ice phase (see Table 3). In order from top to bottom: ice I_h, I_c, III, V and VI. The time at which these instantaneous configurations were taken is 3 μs for the ices I_h and I_c, and 5 μs for the systems formed by ice III, V and VI. Water molecules are plotted in red and white color, Cl^- ions are plotted as green spheres and Na^+ ions as blue spheres. The size of the ions is enlarged with respect to the water molecules for a clearer visualization.

Table 5 Number of water molecules obtained by direct coexistence in the grown ice phase (n_{ice}^{grown}) and the brine phase (n_{water}^{brine}) at the temperature studied (ΔT = −20 K). n_{Cl^-} and n_{Na^+} are the number of dopant ions present in each of the new phases

Ice	n_{ice}^{grown}	$n_{Cl^-}^{ice}$	$n_{Na^+}^{ice}$	n_{water}^{brine}	$n_{Cl^-}^{brine}$	$n_{Na^+}^{brine}$
I_h	5263	15	5	2737	131	141
I_c	5361	13	4	2703	134	143
III	6579	24	29	3789	147	142
V	4773	5	25	3627	125	105
VI	6209	3	14	2431	123	112

Table 6 Dopant concentration (Cl^- and Na^+ ions) in the new doped ice phase and the resulting brine phase at the temperature studied (ΔT = −20 K) for each system (ice/solution) considered in this work. Concentrations are given in mol kg^{-1}

Ice	$m_{Cl^-}^{ice}$	$m_{Na^+}^{ice}$	$m_{Cl^-}^{brine}$	$m_{Na^+}^{brine}$
I_h	0.16	0.05	2.66	2.86
I_c	0.14	0.04	2.75	2.94
III	0.20	0.24	2.15	2.08
V	0.06	0.29	1.91	1.61
VI	0.03	0.12	2.81	2.56

that reported in experimental studies.[42–44] This result indicates that the preferential incorporation is independent of the starting concentration, for different initial solution concentrations (0.599 M in the previous work and 1 M in the present work) the preference is the same, the number of Cl^- ions that is incorporated into the solid lattice is considerably greater than the number of Na^+ ions for the same degree of subcooling (ΔT = −20 K). In our previous work for ice I_h we demonstrated how it was necessary to increase the degree of subcooling (above −15 K) to observe the doping of Na^+ ions and a subcooling of −20 K allowed us to obtain concentrations of ionic species (Cl^- and Na^+) in the ice lattice similar to the experimental values. For this reason, we chose the same degree of subcooling in the present paper.

Ice I_c presents similar results to ice I_h in terms of number of doping ions and preferential incorporation. In both ices, at the same pressure and degree of subcooling, the number of Cl^- ions incorporated in the solid lattice is considerably greater than the number of Na^+ ions. In Table 5 the number of dopant ions present in each of the phases is given. For ice III the situation begins to change, there is a similar amount of Cl^- and Na^+ ions into the solid lattice, revealing that for this ice there is no preference for incorporation of either of the two ions. The number of Cl^- dopants is similar to the number of Na^+ dopants as shown in Fig. 3 and in the Table 5. Surprisingly, for ices V and VI the situation is completely opposite to what one would expect after the study of ice I_h. Now, the ion that is preferentially incorporated into the ice lattice is Na^+. As can be seen in the Table 5, the number of Cl^- ions that are incorporated into the portions of ice V and VI is very small. We have seen therefore that for the ices stable at increasing pressures, the preference for the incorporation of ions gradually changes from Cl^- to Na^+, and then the system points to an almost complete exclusion of both species upon further increasing the pressure as for ice VI both concentrations decrease with respect to ice V. This difference in the preferential incorporation of dopants is an essential finding that could explain different properties and pave the way to new applications for these ice phases.[44,45]

In addition to the growth and doping of the ice phase, the appearance of a brine phase rejected is observed in Fig. 3 for all the systems studied. The volume of the brine phase depends on the growth rate of ice. Thus, in the case of ice I_h, I_c and VI the volume occupied by the brine phase is smaller than in the other systems studied since for ice III and V the final equilibrium state has not been reached. In Table 5 the number of water molecules that form the jet brine phase are also collected.

The concentration of dopants in the portion of ice grown for each system is shown in the Table 6. As reflected in the results, the concentration of dopants is different for each ice. The ices I_h and I_c have a greater concentration of Cl^- ions in the new ice slab and, consequently, a greater concentration of Na^+ ions in the brine phase. Ice III has very similar concentrations for both the Cl^- and Na^+ ions. On the contrary, for the ice V and VI the concentration of Na^+ ions is considerably higher in the ice phase. The concentration of the dopants in the portion of ice, although it is small, cannot be considered negligible and the incorporation of these ions in the solid lattice can modify electrical properties such as static conductivity.[11]

In view of the results, a question arises: is the preferential incorporation (and therefore the concentration of dopants) due to the type of crystalline structure of the ice or to the pressure applied? Our results show that for systems containing ice I_h and I_c and pressure 1 bar, the Cl^- ion has preference in the ice-doping process. For ice III we simulate the system at 3500 bar and both dopants are incorporated into the lattice in a similar proportion. For ice V and VI, at pressures of 7000 bar and 12 000 bar respectively, it is the Na^+ ion that is preferentially incorporated into the slab of doped ice. To solve this issue, we have prepared a similar system to that of ice I_h in contact with a solution of 1 M and we have simulated it at a pressure of 1000 bar for 1.5 microseconds. In Fig. 4 a final snapshot of this system is given and it can be seen as even increasing the pressure the Cl^- is preferentially incorporated into the ice lattice. Thus, the explanation of the preferential incorporation is due to the type of crystalline structure and its availability to accommodate ions in its network. This explanation makes sense since, if the determining factor were the pressure, the ice VI should present a greater concentration of dopants, on the contrary, it is the ice V which has a greater concentration revealing a greater availability to accommodate ions. Fig. 5 shows the comparison of the potential energy as a function of time for the same system (a slab of ice I_h in contact with a solution) at the two different pressures studied and at the same degree of subcooling. Both curves have a very similar slope, showing that the ice growth and the growth rate are similar for the same ice regardless of the applied pressure. In view of the results, we can conclude that the different preferential inclusion is due exclusively to the different crystalline structures and not to the pressure applied along the interface.

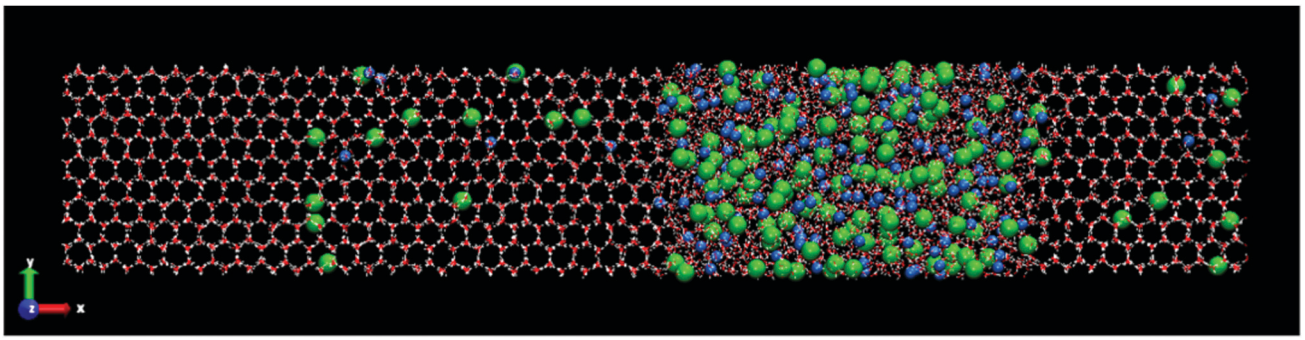

Fig. 4 Snapshot of an instantaneous configuration taken at 1.6 μs of simulation time and obtained by direct coexistence for the system formed by a slab of ice I_h and a NaCl aqueous solution 1 M at (ΔT = −20 K) and p = 1000 bar. Water molecules are plotted in red and white color, Cl^- ions are plotted as green spheres and Na^+ ions as blue spheres. The size of the ions is enlarged with respect to the water molecules for a clearer visualization.

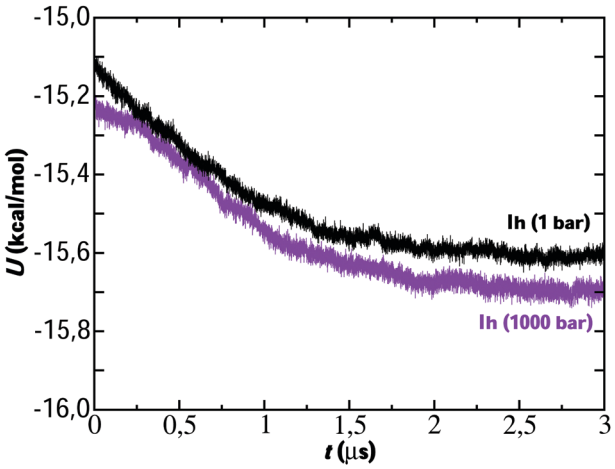

Fig. 5 Comparison of the evolution of the potential energy as a function of the simulation time for the system ice I_h/NaCl(aq) at different pressures. In both cases the simulation was performed at ΔT = −20 K. The pressure to which the direct coexistence simulations have been performed for each simulation run is indicated in parentheses.

Once we have verified that it is possible to dope all the ice phases studied in this work, we are now going to analyze in detail the mechanism of inclusion of the two ionic species for each of the systems studied. For clarity and understanding, we select for each type of ice a small portion of the water molecules in the pure ice lattice to know exactly how these molecules are arranged and oriented and compare it with similar portions where there are Cl^- and Na^+ ions doping the network. These doped portions are taken from the final configurations and obtained in the slabs of new grown ices. For the study of pure ice we take small portions of the ice seed that we put initially and that is equilibrated at the conditions of pressure and temperature of the doped part. We note that our equilibrated configurations do not show the water molecules sitting at the sites of the perfect lattice. Because of finite temperature, the lattice sustains in fact thermal modes of vibration and these cause small misplacements of the molecules in the instantaneous configurations of the systems with respect to the equilibrium positions. In the following discussion, network defects included in the pure ice portion have not been considered. Only the possible defects that the ions can cause by doping the network are considered.

We now show, for each ice, the same portion selected for the pure ice, for the ice in the presence of a Cl^- ion and for the ice in presence of a Na^+ ion.

The crystal structure of pure ice I_h is displayed in the left panels of Fig. 6 and it shows a particular arrangement of the molecules characterized by the presence of large hexagonal channels. The basic structure consists of chair-form hexagonal rings (horizontal plane) or boat-form hexagonal rings (vertical plane). The portion of pure ice selected for our study is composed of 26 water molecules located in two layers of three hexagonal rings each. A front view of the projection of the *xy* plane where the hexagonal channels are clearly observed is shown in Fig. 6 (top left panel). Likewise, we use the *xz*-plane projection to help visualize the ion inclusion mechanisms (bottom left panel). We continue by analyzing what happens to the phase of ice I_h when it is doped by Cl^- ions. Already in our previous work[23] on seawater conditions, we found that Cl^- ions included in the lattice always substitute not one but two water molecules. In the Fig. 6 it is clearly observed how, in both planes, the portion of ice that contains the Cl^- ion presents 24 water molecules, revealing the loss of 2 water molecules replaced by a Cl^- ion with respect to the portion of pure ice. We note also that the lattice is not distorted. This result is in perfect agreement with the results found in the previous study. The loss of water molecules in the lattice also causes the creation of a L-type Bjerrum defect. This type of defect, specific to ice and responsible for the electrical properties of ice,[11,12] basically consists of the creation of a hydrogen bond in the absence of protons. This is the situation that occurs in the vicinity of each Cl^- ion presents in the solid network where a hydrogen bond is created between the Cl^- ion and the oxygen of a neighboring water molecule. The presence of these substitutional defects in ice favors conduction. The inclusion mechanism in the case of Na^+ ion occurs *via* interstitial sites instead, as it is evident from the right panels of Fig. 6. We can see how the Na^+ ion occupies an interstitial site. The presence of Na^+ ions in the solid lattice does not generate the creation of

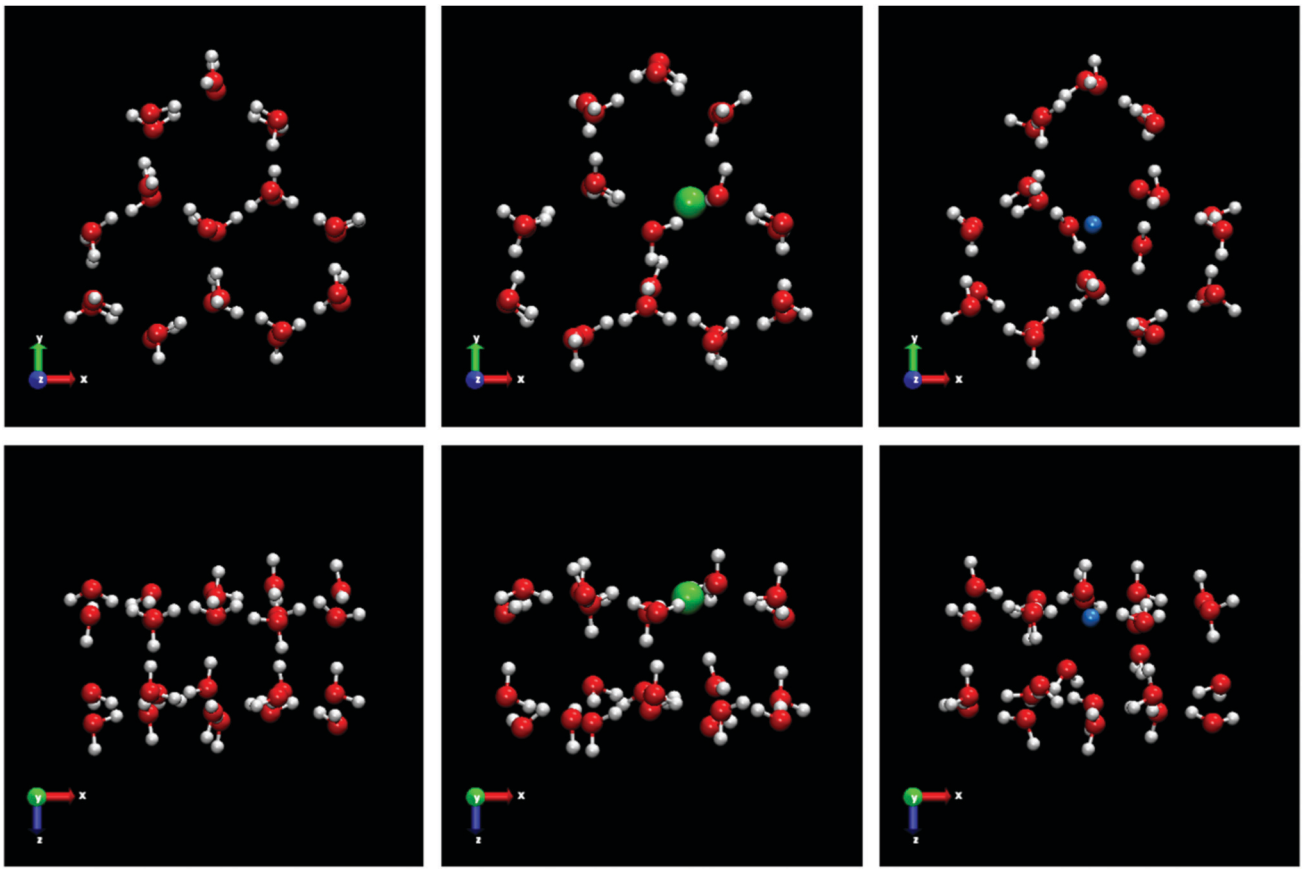

Fig. 6 Visualization of the ion inclusion mechanism in the spontaneous doped slab of ice I_h. Top: Frontal view of the *xy* plane projection of a pure ice I_h lattice portion (left), a portion doped by a Cl^- ion (center) and a portion doped by a Na^+ ion (right). Bottom: Same lattice portions views for the ice I_h on the *xz* plane projection. All doped lattice portions were obtained from the new growth ice phase in the direct coexistence simulations. Water molecules are plotted in red and white color, Cl^- ions are plotted as green spheres and Na^+ ions as blue spheres.

defects although its presence causes a quite relevant local distortion of the ice lattice as can be clearly seen in both planes by the displacement of water molecules when incorporating the Na^+ ion.

To confirm this local distortion of Na^+ ions, we show a study on the positions of the water molecules in the solid network around their equilibrium positions for 10 ns. The instantaneous configurations for the portion of pure ice I_h are collected in Fig. 7. We take every 0.5 ns instantaneous configurations of the portion of pure ice and observe that although small displacements of the water molecules are shown, these are due to movements around the equilibrium position and no local distortion is observed as in the case of the Na^+ dopants.

The inclusion of a Cl^- or Na^+ ion in the ice lattice affects the orientation of the hydrogens in nearby water molecules as a function of the charge on the ion. In the presence of the Cl^- ion, the nearby water molecules are oriented towards the negatively charged ion. On the contrary, the hydrogens move away from the positive charge of the Na^+ ion. These different hydrogen orientations of the water molecules depending on the type of ion accommodated in the ice lattice can be observed in the projections of the *xy* plane of Fig. 6.

Ice I_c is the metastable phase of ice I_h. It is a proton disordered phase. In recent years, this cubic polymorph (ice I_c) has been interpreted not as a pure ice phase but as a structure with mixed cubic/hexagonal stacking.[46,47] However, in 2020, it has been found that pure cubic ice could be produced from ice XVII without stacking defects.[48] Ice I_h and I_c are crystalline structures very alike. Both forms have a very similar density and are open low-density structures. Moreover, both forms contain similar layers of hexagonal rings, but differ in the way these layers are connected. Ices I_h and I_c present an ABABAB and an ABCABC stacking sequence of planes, respectively. Fig. 8 shows the visualization of the inclusion mechanism for ice I_c. Two different projections in the plane have been used to improve the visualization and understanding of the inclusion mechanism. Pure ice I_c portion is composed of 28 water molecules. In the second column of the Fig. 8 a similar portion of ice I_c is shown with a Cl^- ion doping the lattice. It is clearly observed in both projections as Cl^- ion replaces two water molecules. This result is in agreement with the same mechanism found for doped ice I_h. The portion of ice I_c doped by Cl^- ion contains 26 water molecules and 1 Cl^- ion. Since both structures are very similar, this result does not seem surprising. However, when the Na^+ ion dopes the ice lattice, the mechanism of inclusion changes with respect to that found for ice I_h. As can be seen in the Fig. 8 (right column), the Na^+

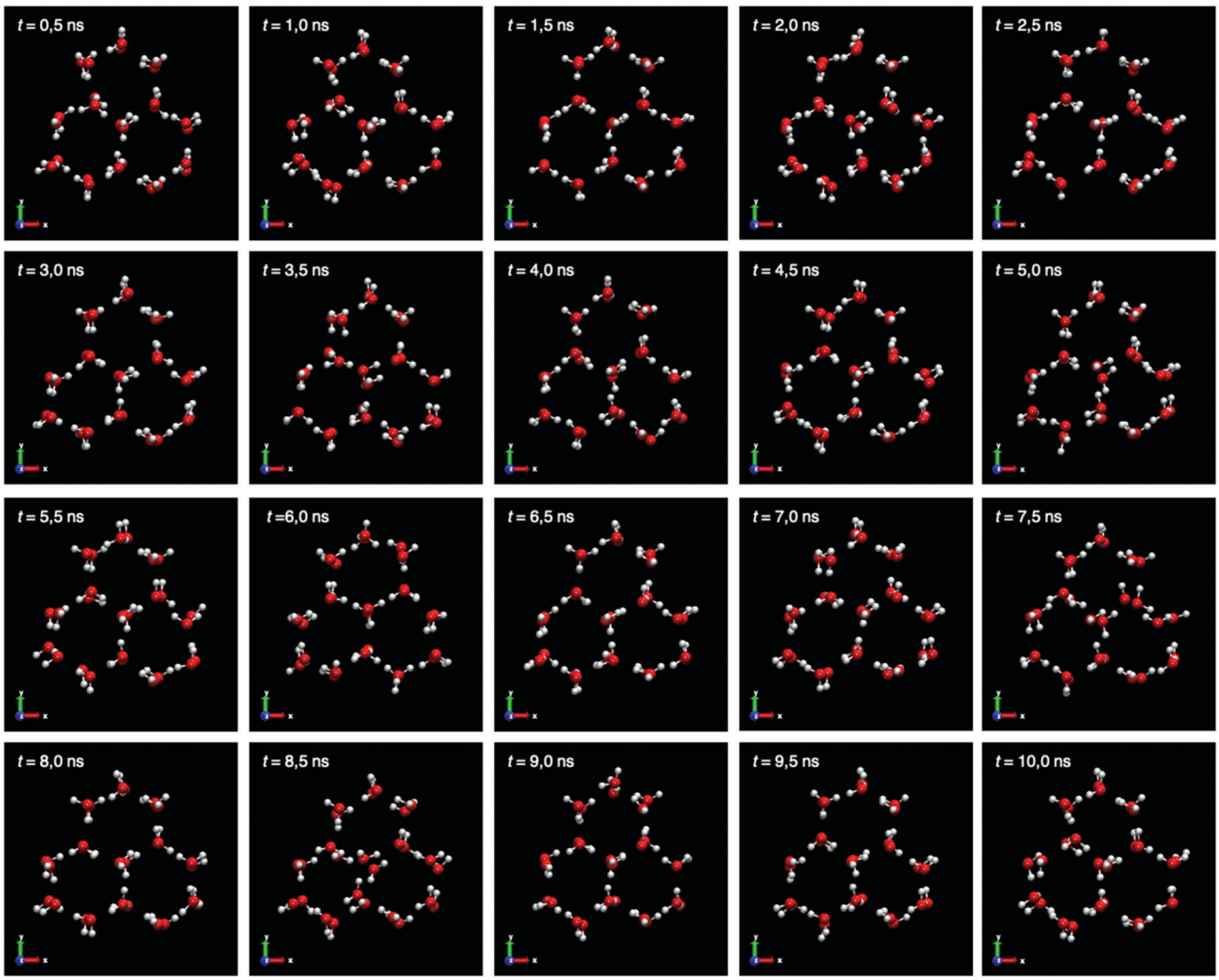

Fig. 7 View of different instantaneous configurations taken along a run of 10 ns, at 0.5 ns intervals, for the same lattice portion of ice I_h. Vibrational movements of the water molecules are observed but no distortion of the portion lattice.

ion replaces a water molecule resulting in the loss of a water molecule with respect to the portion of pure ice I_c. Contrary to ice I_h, in the ice I_c the mechanism of inclusion for the Na^+ ions is a substitutional mechanism.

This difference in the mechanism can be explained through the arrangement of the water molecules in the lattice of ice I_h and ice I_c, especially in the differences in the numbers of water molecules in the hydration shells of both ices. Specifically, in ice I_h cavities are formed by twelve molecules while in ice I_c cavities are smaller and are formed by ten molecules.[49] As ice I_c has smaller cavities, it means that the Na^+ ion does not have space to be located in the interstitials and the substitution by a water molecule is the most favorable mechanism for its inclusion into the lattice. Moreover, while for ice I_h hexagonal rings can have both a chair conformation and a boat conformation, for ice I_c 6-membered rings can adopt only chair conformation. As a consequence of the chair conformation in ice I_c there are no open channels in the direction 111, while in ice I_h they exist as indicated in ref. 11.

Ice III is a complex and high-density phase.[50] It is located in the intermediate pressure zone of the water phase diagram. It is a partial proton disordered phase. All water molecules are hydrogen bonded to four others, two as donor and two as acceptor. Ice III forms tetragonal crystals. Ice III presents a complicated arrangement of five-membered rings of hydrogen bonded molecules with several different bond lengths and angles. As in the previous cases, we use a portion of pure ice to compare the positions of the water molecules when the ions are incorporated into the lattice and thus study the mechanism of inclusion. For ice III, the pure ice portion selected is made up of 28 water molecules. The five-membered rings of ice III are clearly visible in the frontal view of the *xy* plane projection of the Fig. 9. When the ice portion is doped by a Cl^- ion there is a water molecule missing. It is the only one of the ices studied in this work where the Cl^- ion replaces one water molecule and not two water molecules. All the Cl^- ions found for this ice III (see Table 5) follow the same mechanism of substitution of a single water molecule. A possible explanation of these

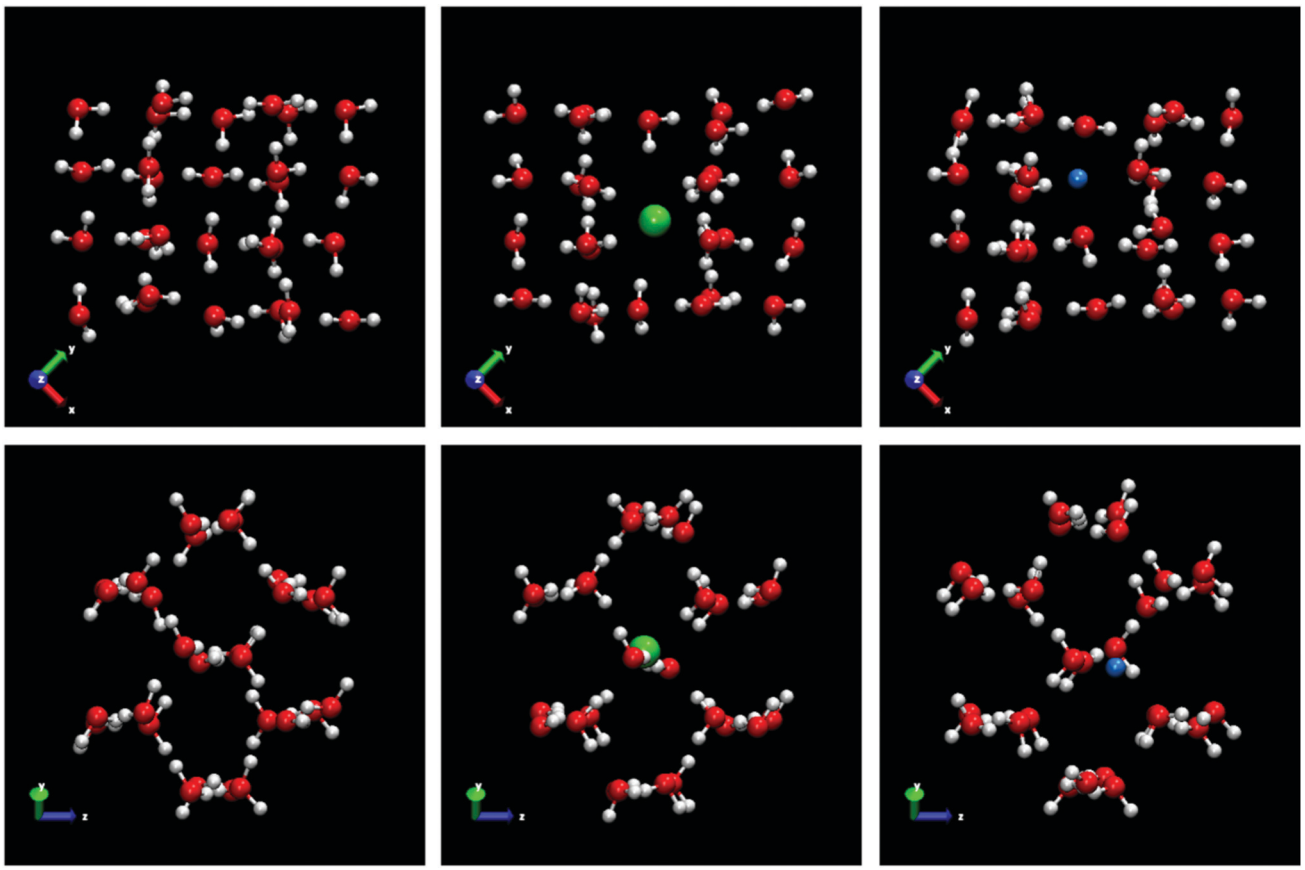

Fig. 8 Visualization of the ion inclusion mechanism in the spontaneous doped slab of ice I_c. Top: Frontal view of the *xy* plane projection of a pure ice I_c lattice portion (left), a portion doped by a Cl^- ion (center) and a portion doped by a Na^+ ion (right). Bottom: Same lattice portions views for the ice I_c on the *z* plane projection. All doped lattice portions were obtained from the new growth ice phase in the direct coexistence simulations. Water molecules are plotted in red and white color, Cl^- ions are plotted as green spheres and Na^+ ions as blue spheres.

differences is due to the arrangement of water molecules in ice and how their different connectivity favors the substitution of one or two water molecules by Cl^- ion. In the case of ice III with 5-membered water molecule rings, and in view of the results obtained, the substitution mechanism of a water molecule is more energetically favorable than the substitution of two water molecules. On the contrary, Na^+ ion occupies an interstitial site and its presence causes a local distortion of the ice lattice similar to the distortion observed in ice I_h by the presence of Na^+ ions. In this portion of ice III doped by the Na^+ ion, the same number of 28 water molecules is maintained as in the portion of pure ice.

Ice V is a very complex structure with a monoclinic unit cell.[51] It is a partially proton disordered phase. Ice V has several types of topologically non-equivalent water molecules. It contains four-, five-, six- and eight-membered rings of water molecules. All molecules form one connected lattice. For the portion of pure ice V we select 18 water molecules. Fig. 10 shows the frontal views of the *xy* and *xz* planes for the portions of pure ice V and for the portions of Cl^-- and Na^+-doped ice. From the portion of ice V doped by Cl^--ion it is clearly observed how the inclusion of an ion in the lattice causes the substitution of two water molecules. The number of molecules in the portion of doped ice by Cl^--ion is 16 water molecules and 1 Cl^--ion. Again, we observe a mechanism of substitution of two water molecules in a solid structure of water. This mechanism was observed in all Cl^--ions that doped the ice phase V studied in this work. Analogously to ice I_h and III, Na^+ ions are located in the interstitial sites resulting in a portion formed by 18 water molecules and 1 Na^+ ion. The Na^+ ion does not appear to cause a local distortion as in the case of ice I_h and III. All portions of ice V (pure and doped) can be seen in Fig. 10.

Ice VI is a full proton disordered phase with tetragonal symmetry.[52] Compared to ice III and ice V, ice VI occupies a large area on the water phase diagram in the high pressure region. Ice VI contains four-member rings of water molecules. The tetragonal unit cell of ice VI is formed by two independent but interpenetrating hydrogen bonded networks. These are two completely separated interpenetrating networks with no connecting hydrogen bond. Besides, in ice VI, not all molecules are topologically equivalent while all the molecules are topologically equivalent in ice I_h. In each sub-lattice, the structure of ice VI is made up of chains of water molecules linked by hydrogen bonding. The portions of ice VI used to elucidate the mechanism of inclusion of Cl^- and Na^+ ions are shown in the Fig. 11. For the portions of ice VI, in the frontal view of the projection of

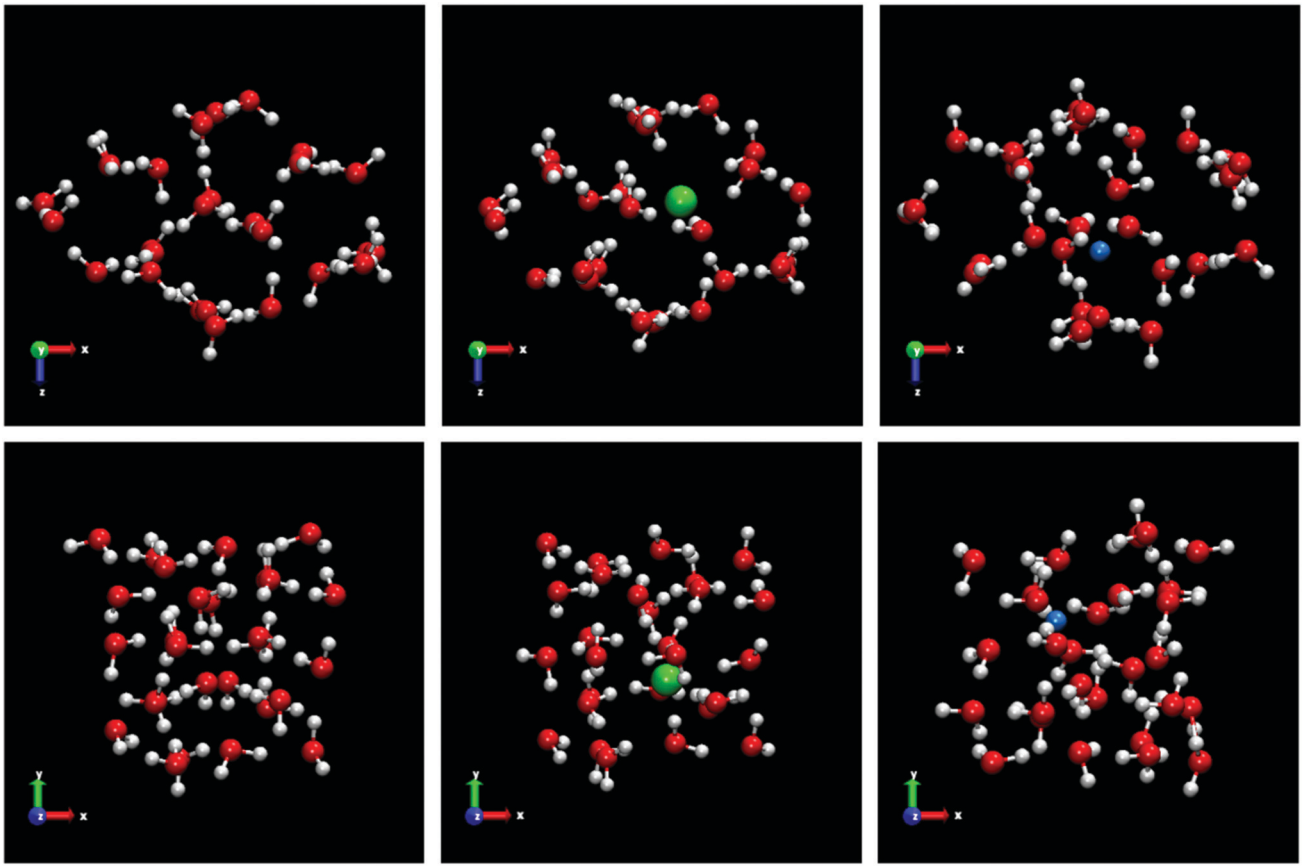

Fig. 9 Visualization of the ion inclusion mechanism in the spontaneous doped slab of ice III. Top: Frontal view of the *xy* plane projection of a pure ice III lattice portion (left), a portion doped by a Cl^- ion (center) and a portion doped by a Na^+ ion (right). Bottom: Same lattice portions views for the ice III on the *xz* plane projection. All doped lattice portions were obtained from the new growth ice phase in the direct coexistence simulations. Water molecules are plotted in red and white color, Cl^- ions are plotted as green spheres and Na^+ ions as blue spheres.

the *xy* plane, it can be clearly seen the 4-membered ring of water molecules from one of the sub-lattices surrounded by water molecules belonging to the other sub-lattice. In the *xz* projection the chains of water molecules linked by hydrogen bonds are observed. The portion of pure ice VI selected is composed of 21 water molecules. As can be seen in the central panel of the Fig. 11, when a Cl^- ion dopes the structure of ice VI, the portion becomes formed by 19 water molecules resulting in the loss of 2 water molecules. As in previous cases for most of the ices studied except for ice III, the mechanism of inclusion of Cl^- ion is through the substitution of two water molecules. As it expected, the substitution of molecules occurs in one of the sub-lattice that form the structure of ice VI. It is not possible to find a Cl^- ion that connects both sub-lattices, the two missing molecules belong to the same sub-lattice, either one or the other. The presence of the Cl^- ion provokes that the hydrogens of the nearby water molecules are oriented toward the ion. For the inclusion of Na^+ ions, the mechanism is similar to that found for most ices. Na^+ ions are incorporated into the solid structure through the interstitial sites causing a slight distortion of the water molecules neighboring the Na^+ ion. In the right panel of the Fig. 11, it can be seen how, due to the presence of the Na^+ ion in the ice VI, the hydrogens of the water molecules close to the Na^+ ion are oriented away from the positive charge of the ion. This phenomenon about the different hydrogen orientations due to the presence of Cl^- or Na^+ ions in the vicinity are found in all ices studied.

Finally, it is important to note that for all the systems studied, dopant ions are obviously located only in the new slab of grown ice and not in the initial ice used as seed crystal. Since for all the ices the Cl^- ions that doped the solid lattice substitute water molecules it is clear that they will remain in their positions in the lattice and will not be exchanged or diffused. As for Na^+ ions located in the interstitial sites, in our previous work we observed small displacements of the Na^+ through the lattice. But since the population of Na^+ ions was very small we could not study this matter in detail. We assume that over time these Na^+ ions will diffuse through the lattice. However our statistics did not allow us to inquiry on the problem of diffusion. In Table 7 a summary of the inclusion mechanisms of each one of the ices studied in this work is shown.

4 Conclusions

In this work we have studied the spontaneous NaCl-doped for different types of ice. We have performed computer simulations

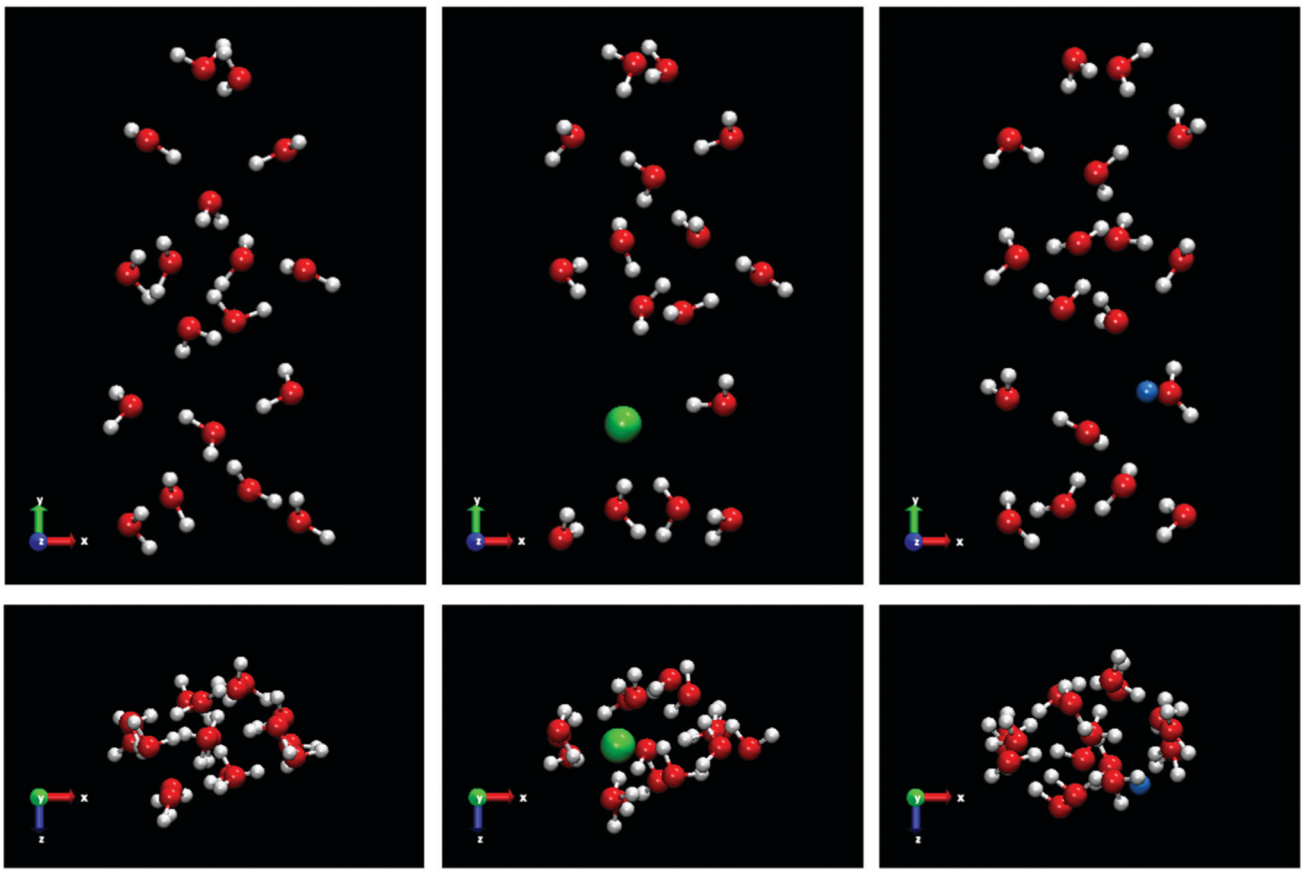

Fig. 10 Visualization of the ion inclusion mechanism in the spontaneous doped slab of ice V. Top: Frontal view of the *xy* plane projection of a pure ice V lattice portion (left), a portion doped by a Cl^- ion (center) and a portion doped by a Na^+ ion (right). Bottom: Same lattice portions views for the ice V on the *xz* plane projection. All doped lattice portions were obtained from the new growth ice phase in the direct coexistence simulations. Water molecules are plotted in red and white color, Cl^- ions are plotted as green spheres and Na^+ ions as blue spheres.

using the direct coexistence technique to analyze the mechanisms of ion inclusion. Additionally, our results show the growth of a new ice-doped phase from NaCl aqueous solution in contact with a solid phase of the different types of ice studied (ice I_h, I_c, III, V and VI). The model used for water is TIP4P/2005.[37] For NaCl we have considered a set of potential parameters that use unit charges for the ions.[38] The main conclusions of this work are as follows:

• For the first time by molecular dynamic simulations, the spontaneous doping by Cl^- and Na^+ ions of all the ices studied is observed. This finding is very significant to explain the behavior of ice in the presence of ionic species as it occurs in planetary conditions.

• Long time simulations on a microsecond time scale are required to produce a slab of doped ice large enough to have a significant number of Cl^- and Na^+ ions doping the newly grown ice.

• In line with the previous results obtained for ice I_h, we also observed the formation of a brine rejection phase in all the ices studied. The growth rate of the ice phase from aqueous solutions is different depending on each ice and slower than the pure phase, following the trend of the growth rates of the pure ices in the absence of salt. The potential energy curves reveal that the time to reach the final state of equilibrium for the systems formed by ice I_h and I_c are considerably shorter than in the rest of the ices where the final state of equilibrium was not reached after 5 microseconds.

• The preferential incorporation of dopants depends exclusively on the crystal ice phase. The pressure applied to the system and the initial salt concentration do not appear to influence the preferential incorporation found for each type of ice.

• It is not possible to speak of a universal inclusion mechanism for the ices doped. Most of the ices studied present a different inclusion mechanism that depends on their crystalline structures.

• For all the ice networks studied, the inclusion of Cl^- ions follows a mechanism of substitution of water molecules causing the appearance of L defects. The number of substituted water molecules depends on the type of ice studied. For most of the ices studied, each Cl^- ion incorporated in the network replaces two water molecules. Only for the system formed by ice III the inclusion of Cl^- ions produces the substitution of a single water molecule. This difference can be explained in terms of the arrangement of the water molecules in the ice crystal lattice. For all the systems studied, we did not observe

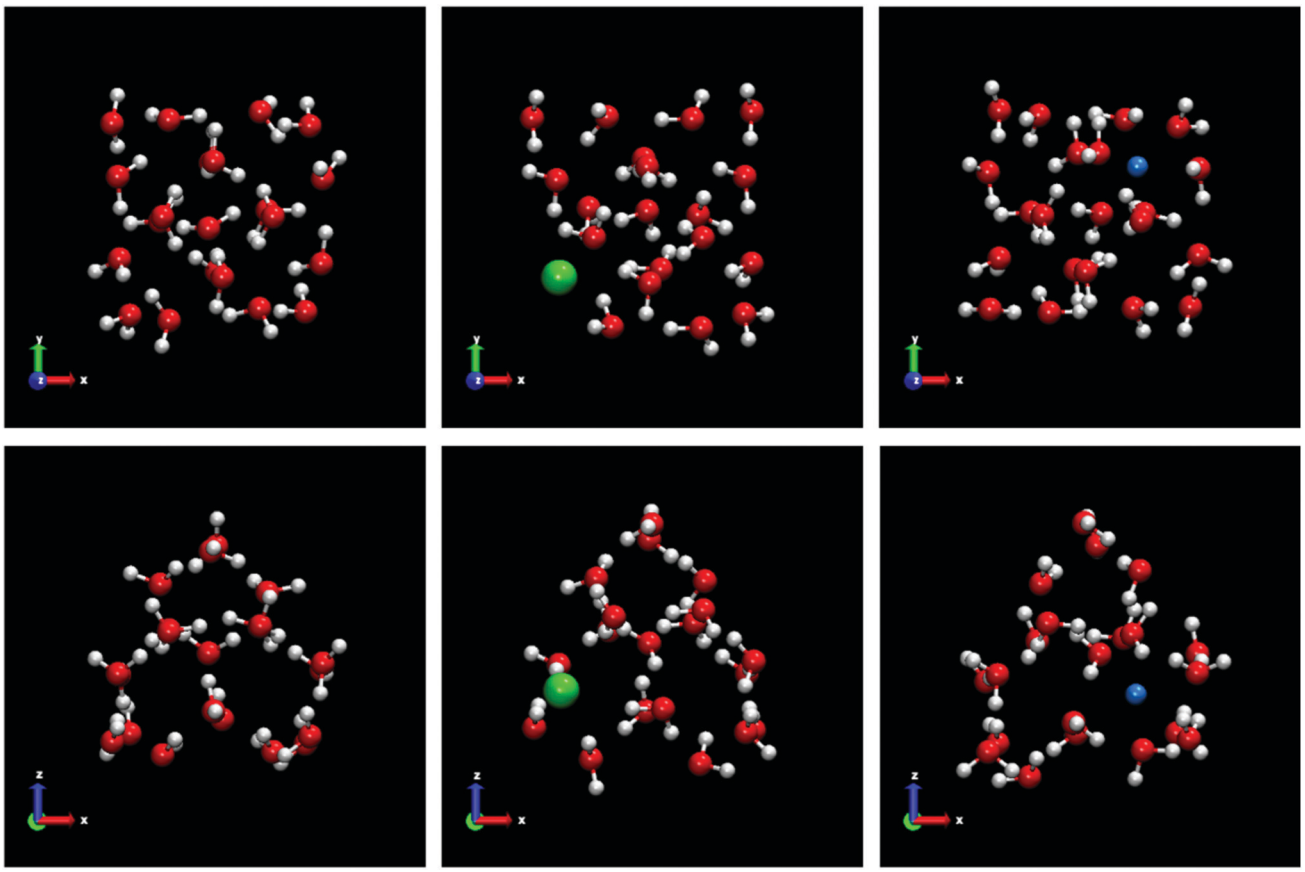

Fig. 11 Visualization of the ion inclusion mechanism in the spontaneous doped slab of ice VI. Top: Frontal view of the *xy* plane projection of a pure ice VI lattice portion (left), a portion doped by a Cl^- ion (center) and a portion doped by a Na^+ ion (right). Bottom: Same lattice portions views for the ice VI on the *xz* plane projection. All doped lattice portions were obtained from the new growth ice phase in the direct coexistence simulations. Water molecules are plotted in red and white color, Cl^- ions are plotted as green spheres and Na^+ ions as blue spheres.

Table 7 Summary of the inclusion mechanisms of each one of the ices studied in this work. The last column collects the number of water molecules substituted when the Cl^- and Na^+ ions dope the ice lattice

Ice	Ion: inclusion mechanism	H_2O subs.
I_h	Cl^-: substitutional	2
	Na^+: interstitial	—
I_c	Cl^-: substitutional	2
	Na^+: substitutional	1
III	Cl^-: substitutional	1
	Na^+: interstitial	—
V	Cl^-: substitutional	2
	Na^+: interstitial	—
VI	Cl^-: substitutional	2
	Na^+: interstitial	—

the distortion of the network due to the incorporation of Cl^- ions.

• In general, Na^+ ions follow an inclusion mechanism through interstitial sites. Ice I_c is an exception for the mechanism of Na^+ ions, in this case, a mechanism of substitution of a single water molecule is found. The presence of Na^+ ions in the solid lattice does not provoke the creation of network defects, although its presence causes a quite relevant local distortion of the ice lattice except for ice I_c where it goes substitutional. The hydrogens of the water molecules close to the Na^+ ion localized at the interstitial sites are oriented away from the positive charge of the ion. On the contrary, hydrogens are oriented towards the negative charge of Cl^- in the vicinity of the ion.

In view of the results obtained, it would be interesting to extend this analysis to other types of dopants to study the effect of different dopants on the inclusion mechanisms and the preferential occupation of the ions in the solid ice network. The temperature of our study can be of relevance for the study of Jovian Satellites that is in progress.[3] When salty solutions become highly concentrated, and their dynamics is slow and glassy, ice does not grow any longer. It would be of interest to see if we can supercool below the eutectic and still have a glassy brine rejection. Finally, in our previous paper[23] we analyzed the Radial Distribution (RDF) of pure ice and doped ice and we found no perturbation in the doped lattice, at least in the RDF, with respect to the perfect lattice. Nonetheless the number of ions is very low so that we have a low statistic in the RDF. Thus, in the future we intend to study the local order in the vicinity of the few ions incorporated into the ice to investigate possible local deformations of the lattice.

Author contributions

All authors contributed equally to all the roles.

Conflicts of interest

There are no conflicts to declare.

Acknowledgements

This work was funded by Grant No. PID2019-105898GA-C22 of the MICINN and by Project No. ETSII-UPM20-PU01 from "Ayudas Primeros Proyectos de la ETSII-UPM". M. M. C. acknowledges CAM and UPM for financial support of this work through the CavItieS project no. APOYO-JOVENES-01HQ1S-129-B5E4MM from "Accion financiada por la Comunidad de Madrid en el marco del Convenio Plurianual con la Universidad Politecnica de Madrid en la linea de actuacion estimulo a la investigacion de jovenes doctores". The authors gratefully acknowledge the Universidad Politecnica de Madrid (www.upm.es) for providing computing resources on Magerit Supercomputer.

Notes and references

1 M. R. Frank, C. E. Runge, H. P. Scott, S. J. Maglio, J. Olson, V. B. Prakapenka and G. Shen, *Phys. Earth Planet. Inter.*, 2006, **155**, 152.
2 B. Journaux, I. Daniel, R. Caracas, G. Montagnac and H. Cardon, *Icarus*, 2013, **226**, 355.
3 E. Pettinelli, B. Cosciotti, F. D. Paolo, S. E. Lauro, E. Mattei, R. Orosei and G. Vannaroni, *Rev. Geophys.*, 2015, **53**, 593.
4 B. Brugger, O. Mousis, M. Deleuil and J. I. Lunine, *Astrophys. J., Lett.*, 2015, **831**, L16.
5 K. Aagaard and E. C. Carmack, *J. Geophys. Res.*, 1989, **94**, 14485.
6 A. Y. Shcherbina, L. D. Talley and D. L. Rudnick, *Science*, 2003, **302**, 1952.
7 K. I. Ohshima, Y. Fukamachi, G. D. Williams, S. Nihashi, F. Roquet, Y. Kitade, T. Tamura, D. Hirano, L. Herraiz-Borreguero, I. Field, M. Hindell, S. Aoki and M. Wakatsuchi, *Nat. Geosci.*, 2013, **6**, 235.
8 I. Tsironi, D. Schlesinger, A. Spah, L. Eriksson, M. Segad and F. Perakis, *Phys. Chem. Chem. Phys.*, 2020, **22**, 7625.
9 M. Conde, M. Rovere and P. Gallo, *J. Mol. Liq.*, 2018, **261**, 513–519.
10 J. S. Kim and A. Yethiraj, *J. Chem. Phys.*, 2008, **129**, 124504.
11 V. F. Petrenko and R. W. Whitworth, *Physics of Ice*, Oxford University Press, 1999.
12 N. Bjerrum, *Science*, 1952, **115**, 385–390.
13 G. W. Gross, *Ann. N. Y. Acad. Sci.*, 1965, **125**, 380.
14 G. W. Gross, *Adv. Chem.*, 1968, **73**, 27.
15 A. W. Cobb and G. W. Gross, *J. Electrochem. Soc.*, 1969, **116**, 796.
16 C. Jaccard, *Ann. N. Y. Acad. Sci.*, 1965, **125**, 390–400.
17 I. G. Young and R. E. Salomon, *J. Chem. Phys.*, 1968, **48**, 1635–1644.
18 D. J. Kelly and R. E. Salomon, *J. Chem. Phys.*, 1969, **50**, 75–79.
19 R. G. Seidensticker and R. L. Longini, *J. Chem. Phys.*, 1969, **50**, 204–213.
20 S. Klotz, L. E. Bove, T. Strässle, T. C. Hansen and A. M. Saitta, *Nat. Mater.*, 2009, **8**, 405.
21 L. E. Bove, R. Gaal, Z. Raza, A. A. Ludl, S. Klotz, A. M. Saitta, A. F. Goncharov and P. Gillet, *Proc. Natl. Acad. Sci. U. S. A.*, 2015, **112**, 8216.
22 V. Rozsa and G. Galli, *J. Chem. Phys.*, 2021, **154**, 144501.
23 M. M. Conde, M. Rovere and P. Gallo, *Phys. Chem. Chem. Phys.*, 2017, **19**, 9566.
24 M. M. Conde, M. Gonzalez, J. Abascal and C. Vega, *J. Chem. Phys.*, 2013, **139**, 154505.
25 M. M. Conde, M. Rovere and P. Gallo, *J. Chem. Phys.*, 2017, **147**, 244506.
26 A. Zaragoza, M. M. Conde, J. R. Espinosa, C. Valeriani, C. Vega and E. Sanz, *J. Chem. Phys.*, 2015, **143**, 134504.
27 H. Nada and Y. Furukawa, *J. Cryst. Growth*, 2005, **283**, 242.
28 M. M. Conde, C. Vega and A. Patrykiejew, *J. Chem. Phys.*, 2008, **129**, 014702.
29 J. R. Espinosa, E. Sanz, C. Valeriani and C. Vega, *J. Chem. Phys.*, 2013, **139**, 144502.
30 V. Buch, P. Sandler and J. Sadlej, *J. Phys. Chem. B*, 1998, **102**, 8641.
31 J. D. Bernal and R. H. Fowler, *J. Chem. Phys.*, 1933, **1**, 515.
32 D. Frenkel, *Eur. Phys. J. Plus*, 2013, **128**, 10.
33 D. van Der Spoel, E. Lindahl, B. Hess, G. Groenhof, A. E. Mark and H. J. C. Berendsen, *J. Comput. Chem.*, 2005, **26**, 1701.
34 S. Nosé, *J. Chem. Phys.*, 1984, **81**, 511.
35 W. G. Hoover, *Phys. Rev. A: At., Mol., Opt. Phys.*, 1985, **31**, 1695.
36 M. Parrinello and A. Rahman, *J. Appl. Phys.*, 1981, **52**, 7182.
37 J. L. F. Abascal and C. Vega, *J. Chem. Phys.*, 2005, **123**, 234505.
38 C. Vega, 2016, private communication.
39 A. L. Benavides, M. A. Portillo, V. C. Chamorro, J. R. Espinosa, J. L. F. Abascal and C. Vega, *J. Chem. Phys.*, 2017, **147**, 104501.
40 I. M. Zeron, J. L. F. Abascal and C. Vega, *J. Chem. Phys.*, 2019, **151**, 134504.
41 U. Essmann, L. Perera, M. L. Berkowitz, T. Darden, H. Lee and L. G. Pedersen, *J. Chem. Phys.*, 1995, **103**, 8577.
42 N. Maeno, *Can. J. Phys.*, 1973, **51**, 1045.
43 G. W. Gross, I. C. Hayslip and R. N. Hoy, *J. Glaciol.*, 1978, **21**, 143.
44 N. W. Riley, G. Noll and J. W. Glen, *J. Glaciol.*, 1978, **21**, 501.
45 R. E. Grimm, D. E. Stillman, S. F. Dec and M. A. Bullock, *J. Phys. Chem. B*, 2008, **112**, 15382.
46 T. L. Malkin, B. J. Murray, A. V. Brukhno, J. Anwar and C. G. Salzmann, *Proc. Natl. Acad. Sci. U. S. A.*, 2012, **109**, 1041.
47 W. F. Kuhs, C. Sippel, A. Falenty and T. C. Hansen, *Proc. Natl. Acad. Sci. U. S. A.*, 2012, **109**, 21259.
48 L. del Rosso, M. Celli, F. Grazzi, M. Catti, T. C. Hansen, A. D. Fortes and L. Ulivi, *Nat. Mater.*, 2020, **19**, 663.
49 http://www.lsbu.ac.uk/water/.
50 B. Kamb and A. Prakash, *Acta Crystallogr., Sect. B: Struct. Crystallogr. Cryst. Chem.*, 1968, **24**, 1317.
51 B. Kamb, A. Prakash and C. Knobler, *Acta Crystallogr.*, 1967, **22**, 706.
52 B. Kamb, *Science*, 1965, **150**, 205.